

Parameters influencing the outcome after total disc replacement at the lumbosacral junction. Part 1: misalignment of the vertebrae adjacent to a total disc replacement affects the facet joint and facet capsule forces in a probabilistic finite element analysis

A. Rohlmann · S. Lauterborn · M. Dreischarf ·
H. Schmidt · M. Putzier · P. Strube · T. Zander

Received: 27 April 2013 / Revised: 6 June 2013 / Accepted: 10 July 2013 / Published online: 20 July 2013
© Springer-Verlag Berlin Heidelberg 2013

Abstract

Purpose After total disc replacement with a ball-and-socket joint, reduced range of motion and progression of facet joint degeneration at the index level have been described. The aim of the study was to test the hypothesis that misalignment of the vertebrae adjacent to the implant reduces range of motion and increases facet joint or capsule tensile forces.

Methods A probabilistic finite element analysis was performed using a lumbosacral spine model with an artificial disc at level L5/S1. Misalignment of the L5 vertebra, the gap size of the facet joints, the transection of the posterior longitudinal ligament, and the spinal shape were varied. The model was loaded with pure moments.

Results Misalignment of the L5 vertebra reduced the range of motion up to 2°. A 2-mm displacement of the L5 vertebra in the anterior direction already led to facet joint forces of approximately 240 N. Extension, lateral bending, and axial rotation caused maximum facet joint forces between 280 and 380 N, while flexion caused maximum forces of approximately 200 N. A 2-mm displacement in the posterior direction led to capsule forces of approximately 80 N. Additional moments increased the maximum facet capsule forces to values between 120 and 230 N.

Conclusions Misalignment of the vertebrae adjacent to an artificial disc strongly increases facet joint or capsule

forces. It might, therefore, be an important reason for unsatisfactory clinical results. In an associated clinical study (Part 2), these findings are validated.

Keywords Total disc replacement · Misalignment · Facet joint degeneration · Finite element analysis · Probabilistic

Introduction

Total disc replacement (TDR) is one option for the treatment of lumbar degenerative disc disease. It is thought that artificial discs relieve pain and restore normal range of motion (RoM) [1–4]. However, facet joint degeneration (FJD) at the index level has been reported following TDR [5–7]. Although FJD is associated with pain, the etiology of FJD is still unexplained.

In a retrospective study that included 32 patients with 41 TDRs (ProDisc II), Park et al. [5] observed a progression of FJD in 12 of the 41 implant levels (29 %) after a minimum 2-year follow-up. In contrast, among 47 adjacent segments, the progression of FJD was found in only three levels. In a retrospective study, Shim et al. [6] compared the Charité III disc prosthesis with the ProDisc II prosthesis at a minimum of 3 years postoperatively. The Charité III disc was implemented in 33 patients and the ProDisc II in 24 patients; the degeneration rates of facet joints at the index level were 36 and 32 %, respectively. The rates were not significantly different between the two groups.

In a prospective study, Siepe et al. [7] investigated the fate of facet joints after TDR in 93 patients. In 20 % of the facet joints, progressive FJD was observed. They found FJD more frequently at the index levels than at the non-index levels. The RoM in segments with progressive FJD

A. Rohlmann (✉) · S. Lauterborn · M. Dreischarf ·
H. Schmidt · T. Zander
Julius Wolff Institute, Charité-Universitätsmedizin Berlin,
Augustenburger Platz 1, 13353 Berlin, Germany
e-mail: antonius.rohlmann@charite.de

M. Putzier · P. Strube
Center for Musculoskeletal Surgery, Clinic for Orthopaedics,
Charité-University Medicine Berlin, Berlin, Germany

was significantly lower than in segments that were not affected by any progression of FJD. Furthermore, the progression of FJD negatively affected the postoperative outcome parameters of the visual analogue scale and the Oswestry disability index; this effect was already detected a few months after surgery.

During TDR surgery, part of the degenerated intervertebral disc is removed, and the assembled artificial disc is driven into the resulting space using an anterior approach. The upper plate of the artificial disc is fixed to the cranial vertebra, and the lower plate is fixed to the caudal one. When inserting an artificial disc, the resistance of the two adjacent vertebrae against displacement in the posterior direction is not necessarily the same. The resistance depends on several factors that are related to anatomy or the surgical procedure, such as the stiffness of the adjacent discs, preparation of the implant bed, and differences in the sclerosis of the endplates. Thus, it is possible that due to the insertion the relative alignment in the sagittal plane of the vertebrae adjacent to the implant is altered. This would affect the gap size in the facet joints at the index level and, therefore, the contact facet joint forces and the capsule tensile forces.

We hypothesized (1) that anterior displacement of the cranial vertebra adjacent to a TDR with a ball-and-socket joint relative to the caudal vertebra leads to a reduced facet joint gap and thus higher forces (2) that posterior displacement leads to higher capsule forces, and (3) that displacement in either direction leads to a reduced RoM at the index level. It is assumed that permanent, high facet joint forces and high capsule forces lead to a progression of FJD and thus to a worse clinical outcome.

The aims of this study (part one) were to test our above-mentioned hypotheses using the finite element method, to deliver an explanation of the progression of FJD after TDR, and to determine the factors with the strongest effect on facet joint and facet capsule forces during TDR. In an associated paper (part two), clinical results after TDR are investigated, and the correlation between misalignment of the adjacent vertebrae and clinical outcome is determined to clinically validate our hypotheses.

Methods

Finite element model of the lumbosacral spine

A finite element model of the lumbosacral spine was employed. It has previously been validated regarding intersegmental rotations and intradiscal pressure using experimental data [8–10]. The model consists of five lumbar vertebrae, a sacrum, five intervertebral discs, and all eight major ligaments (Fig. 1a). The facet joints consist of two curved articulating surfaces with anatomical

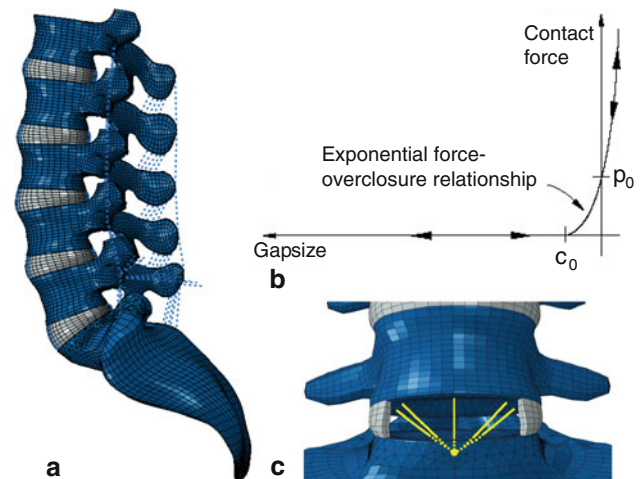


Fig. 1 Finite element model of the lumbosacral spine. **a** Intact model, **b** exponential curve describing the relationship between contact facet joint force and gap size, **c** segment L5/S1 with a kinematic model of total disc replacement

orientation [11]. The cartilaginous layers were simulated using a soft contact with an exponentially increasing contact force and a decreasing contact gap [12] (Fig. 1b). The facet joints had a gap of 0.5 mm in the unloaded neutral position. The annulus fibrosus of an intervertebral disc was modeled as a fiber-reinforced hyperelastic composite [13]. The fibers were embedded in the ground substance and arranged in concentric rings around the nucleus pulposus in 14 layers with a crisscross pattern. The nucleus pulposus was assumed to be incompressible and was modeled as a fluid-filled cavity. The ligaments were represented as tension-only spring elements with a nonlinear force–deflection behavior. More detailed information about the fibers and the ligaments has been presented elsewhere [14–16]. The material properties of the different tissues were taken from the literature and are summarized in Table 1.

Spinal shape

Roussouly et al. [17] measured several parameters (sacral slope, pelvic incidence, pelvic tilt, inflection point, lordosis tilt angle, angle of global lordosis, number of lordotic vertebrae, position of the apex, and the angle and number of vertebrae in the upper and lower arc of lordosis) in lateral X-rays of 160 patients and defined a four-part classification scheme of sagittal morphology. Accordingly, four additional finite element models were created representing these four spinal shapes (Fig. 2).

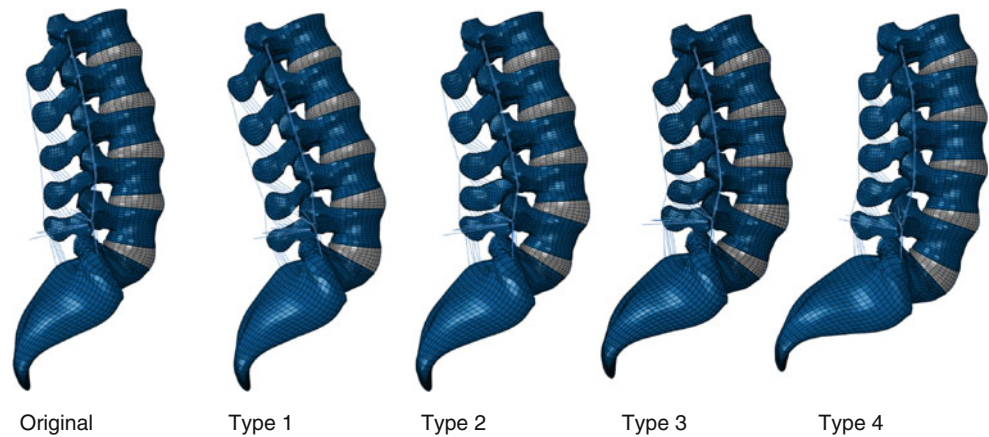
Finite element model with an artificial disc

An artificial disc with one fixed center of rotation (similar to a ProDisc) was implemented in all five models at level

Table 1 Material properties and element types used for the different tissues of the intact model

Component	Elastic modulus (MPa)	Poisson ratio (—)	Element type	References
Cortical bone	10,000	0.30	8-Node Hex	[15, 27]
Cancellous bone, healthy (transverse isotropic)	200/140	0.45/0.315	8-Node Hex	[28]
Posterior bony elements	3,500	0.25	8-Node Hex	[16]
Ground substance of annulus fibrosus	Hyperelastic, neo-Hookean $C_{10} = 0.3448$, $D_1 = 0.3$		8-Node Hex	[13]
Fibers of annulus fibrosus	Nonlinear and dependent on the distance from the disc center		Rebar	[16]
Nucleus pulposus	Incompressible		Fluid	[15, 29]
Ligaments	Nonlinear		Spring	[14, 15]
Cartilage of facet joint	Soft contact			[12]

Fig. 2 Finite element models representing the original model (*left*) and the different types of spinal shapes, after Roussouly et al. [17]. The models vary regarding sacral slope, lordosis tilt angle, angle of global lordosis, number of lordotic vertebrae, inflection point, position of the apex, and the angle and number of vertebrae in the upper and lower arc of lordosis



L5/S1 in the central position (Fig. 1c). For this procedure, the anterior longitudinal ligament was transected, and the nucleus and the anterior part of the annulus fibrosus were removed. The artificial disc was modeled by a kinematical coupling of the adjacent vertebrae [18–20], simulating idealized behavior of the implant. This method was realized with connector elements, which keep the nodes of the adjacent endplates within the allowed kinematics.

Probabilistic study

The following four parameters were simultaneously and uniformly randomized:

- Misalignment of the L5 vertebra in the anteroposterior (a.p.) direction due to implantation of the artificial disc: values of the misalignment varied between -2 and $+2$ mm. The implant position relative to the sacrum was fixed. The L5 vertebra was displaced relative to the upper endplate of the artificial disc in the a.p. direction without constraints. This generally causes forces in the facet joints or in the ligaments and thus leads to an additional rotation of the L5 vertebra in the sagittal plane.
- Resection of the posterior part of the annulus in combination with transection of the posterior longitudinal ligament at level L5/S1: yes or no.

- Spinal shape: five different shapes were investigated; the shape of our original model and the shapes of the four types, after Roussouly et al. [17].
- Initial facet joint gap size: the gap size was varied between 0.3 and 0.7 mm.

The Latin hypercube sampling method [21] was used to generate samples of the four input parameters. The optiSLang (Dynardo, Weimar, Germany) program was employed to randomize the samples and subsequently calculate the probabilistic and sensitivity results. In this study, 400 samples were generated, and thus 400 finite element calculations were performed for each loading case using the finite element program ABAQUS, version 6.8 (SIMULIA Inc. Providence, Rhode Island, USA). This sample size includes a sufficient number of calculations to establish acceptable confidence intervals at the confidence level of 95 %.

The output parameters of the probabilistic finite element study were the intervertebral rotation Cardan angles calculated in the loading plane, the contact forces in the facet joints at the index level and the level above, and the tensile forces in the facet capsule.

Boundary and loading conditions

The caudal part of the sacrum was rigidly fixed. In the first loading step, misalignment of the L5 vertebra in the a.p.

direction was simulated without an additional external load. In the second step, pure moments were applied to simulate motions in the three anatomical main planes. Flexion and extension were simulated by applying bending moments of ± 7.5 Nm in the sagittal plane [22]. For lateral bending, a moment of 8 Nm and for axial rotation, a torsional moment of 5.5 Nm were applied [23, 24].

Evaluation

For the output parameters, scatter diagrams were generated. The RoM, which indicates the overall motion in the loading plane due to the application of a pure moment in both directions, was calculated for flexion–extension, lateral bending, and axial rotation at the index level. Lateral bending and axial rotation caused different loads in the left and right facet joint and facet capsule. If not mentioned otherwise, the higher value is always shown in this study. In a sensitivity study, the coefficient of importance (CoI) was calculated for each of the input parameters. This value reflects the influence of a single input parameter on the output variability. High CoI values, therefore, signify the significant importance of a certain input parameter. A positive value for the a.p. displacement of the L5 vertebra represents an anterior shift of the vertebra relative to the sacrum, while a negative value corresponds to a posterior shift of the L5.

Results

Intervertebral rotation and intervertebral RoM

Without an external load, increased anterior displacement of the L5 vertebra leads to increased extension at the index level, while displacement in the posterior direction has only a minor effect on intervertebral rotation at the index level (Fig. 3). Displacement of the L5 vertebra by ± 2 mm in the a.p. direction causes a change in the intervertebral rotation of approximately 3° . For the loading case flexion, the intervertebral rotation varied between 2.1° and 5.8° . For extension, the displacement variation led to a change in the rotation of up to approximately 2° .

For all principal motions, the RoMs are maximal for little or no L5 misalignment. Increased misalignment in the anterior and posterior direction decreases the RoM at the index level (Fig. 4). For a single spinal shape, the reduction of RoM is maximal for flexion/extension and reaches 2° . There is a larger variation in the results with anterior misalignment.

The RoM of the segment above the TDR is only slightly affected by misalignment at the L5/S1 level.

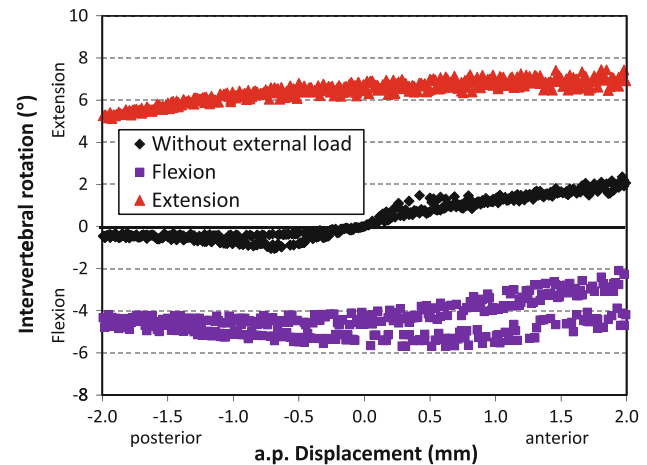


Fig. 3 Effect of an a.p. displacement of the L5 vertebra on intervertebral rotation

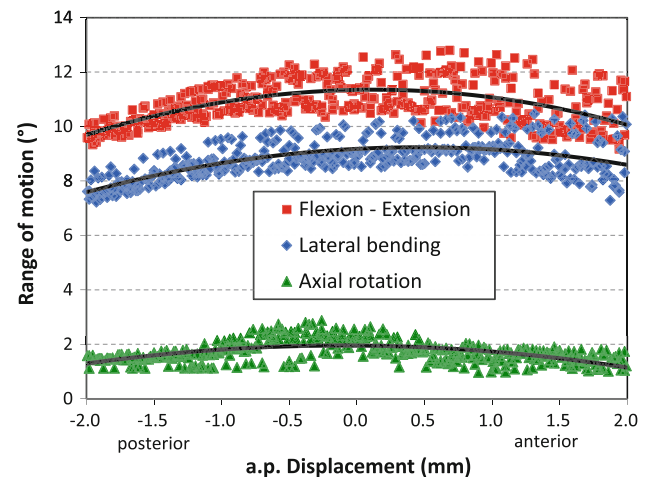


Fig. 4 Effect of an a.p. displacement of the L5 vertebra on intervertebral range of motion in the main anatomical planes. The trendlines have their maximum value for small a.p. displacements

Contact facet joint forces and facet capsule tensile forces at the index level

For values between 0.5 and 2 mm, an anterior L5 misalignment without an external load already leads to contact facet joint forces with maximal values of up to 240 N (Fig. 5). In contrast, the capsular tensile force increases nonlinearly to 20 N for posterior L5 displacements between 0.5 and 1.1 mm (Fig. 6). A further displacement in the posterior direction increases the capsular forces almost linearly up to 80 N.

Flexion in general reduces the facet joint forces, which results from the anterior L5 misalignment (Fig. 5). However, maximum forces of more than 200 N are still predicted. For flexion, the tensile forces in the facet capsule are 20 N without a.p. displacement and reach a value of 160 N for a posterior displacement of 2 mm (Fig. 6).

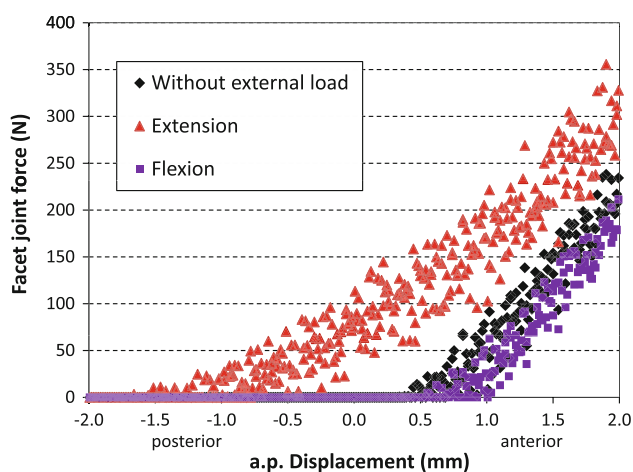


Fig. 5 Influence of an a.p. displacement on contact facet joint forces for the load cases without external load, flexion, and extension

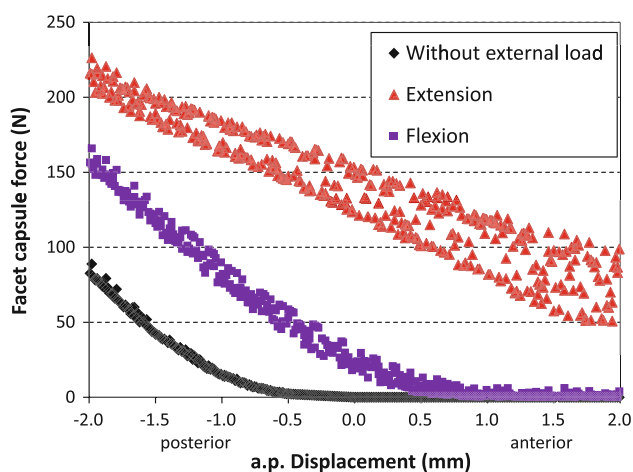


Fig. 6 Effect of an a.p. displacement on facet capsule tensile forces for the load cases without external load, flexion, and extension

Extension increases the facet joint forces (Fig. 5). No contact forces during extension were calculated for an L5 displacement of more than approximately 1.5 mm in the posterior direction. Forces of up to 350 N are predicted for an anterior displacement of 2 mm. The tensile forces in the facet capsule depend almost linearly on the displacement (Fig. 6). An anterior L5 misalignment of 2 mm leads to an average force of approximately 75 N, while this force increases to 220 N for a displacement of 2 mm in the posterior direction.

For lateral bending, forces in the ipsilateral facet joint are predicted for misalignment between 1.2 mm in the posterior and 2 mm in the anterior direction. There is an almost linear increase in the facet joint force with increasing anterior displacement. A maximum value of nearly 400 N is calculated in the present study (Fig. 7). In the facet capsule, tensile forces between 20 and 100 N are predicted for displacements in the anterior direction and a

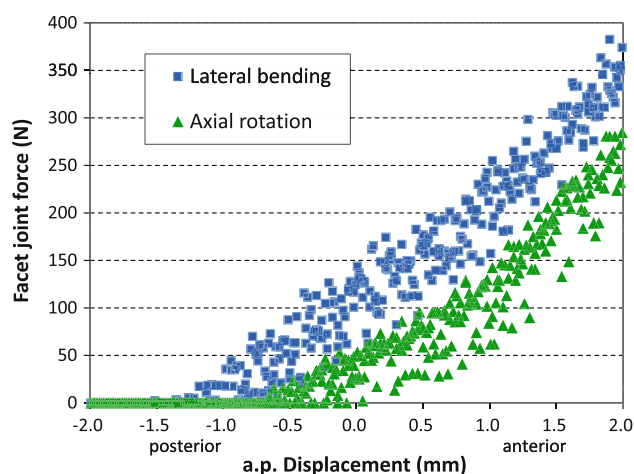


Fig. 7 Influence of an a.p. displacement on contact facet joint forces for lateral bending and axial rotation

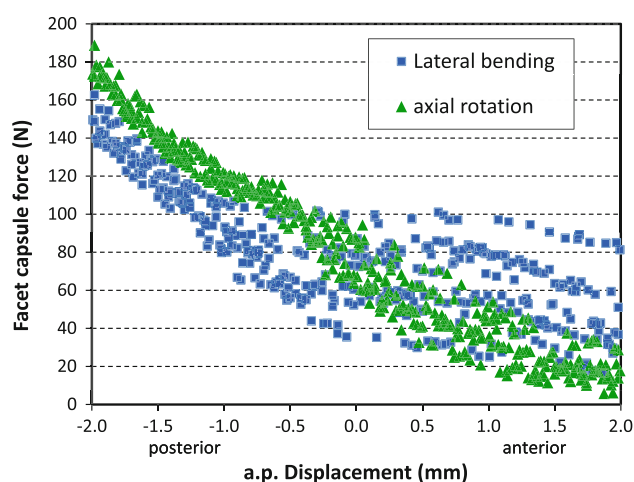


Fig. 8 Effect of an a.p. displacement on facet capsule tensile forces for lateral bending and axial rotation

maximum force of 160 N for a posterior displacement of 2 mm (Fig. 8).

For axial rotation, the calculated facet joint forces are nearly 300 N for an anterior displacement of 2 mm (Fig. 7). In the facet capsule, the maximum tensile force on the contralateral side is approximately 190 N (Fig. 8).

A misalignment at the L5/S1 level has only a minor effect on the facet joint forces and capsular tensile forces in the segments above the TDR.

Coefficient of importance (CoI)

The sensitivity study showed that the misalignment of the L5 has by far the greatest effect on the facet joint forces (Table 2). This parameter explains 53 % of the contact force variation for flexion and 89 % for extension. For lateral bending and axial rotation, the CoIs were 92 and

Table 2 Adjusted Coefficients of Importance (CoIs) in %

Output parameter	Input parameter	Load case				
		Unloaded	Flexion	Extension	Lateral bending	Axial rotation
Contact facet joint force	Spine shape	0	1	0	1	1
	Resection	0	1	0	0	0
	Gap size	1	1	2	2	2
	Misalignment	60	53	89	92	80
Facet capsule tensile force	Spine shape	0	0	0	14	0
	Resection	0	0	7	18	0
	Gap size	0	0	0	0	1
	Misalignment	59	87	91	82	95

Maximum values from the right and left sides are given

Bold CoIs > 80 %

80 %, respectively. The other parameters can explain only up to 2 % of the variance for the different loading cases.

For the capsule tensile forces, the misalignment is the dominant factor (Table 2). For flexion, extension, lateral bending, and axial rotation, CoIs of 87, 91, 82, and 95 %, respectively, were calculated. The other input parameters have CoIs of not more than 7 % for extension, up to 18 % for lateral bending, and a maximum of 1 % for axial rotation.

Discussion

In a probabilistic finite element study with subsequent sensitivity analysis, it could be shown that a misalignment of the L5 vertebrae due to the implantation of a TDR leads to high contact facet joint forces or high tensile forces in the facet capsule and to a decrease in the RoM.

Siepe et al. [7] found lower RoMs during flexion–extension in a cohort of patients with progressive facet joint degeneration in comparison with a group of patients without any progressive degenerative changes. The difference of the medians between the two groups was approximately 3°. For a 2-mm displacement, the current model predicted a reduction of the RoM during flexion–extension of approximately 2° on average. Misalignment of the L5 vertebra was not quantified in any clinical study, and, therefore, maximal values of the anterior and the posterior displacement were estimated in this study. However, the displacement might be even larger than 2 mm after TDR, explaining the slightly larger reduction of the RoM during flexion–extension measured by Siepe et al. [7]. Furthermore, this study shows that besides flexion–extension, there is a reduction of the RoM in all main anatomical planes. This general finding illustrates the overall meaning of a misalignment for the motion and the resultant forces in the facet joint and the capsular ligaments at the index level during daily activities.

For all loading cases studied, an anterior displacement of the L5 vertebra leads to more than 200 N higher facet joint forces (Figs. 5, 7). It is assumed that such a strong load increase may lead to a degeneration of the facet joints, especially because none of the standard loading cases releases the facet joint. The high contact force in one facet joint is for unsymmetrical loading cases accompanied by high facet capsule tensile forces in the other facet joint. Additionally, for a posterior displacement, high facet capsule forces are predicted. These high tensile forces may also cause local effects, which might accelerate the degeneration process in the facet joint. The results of this study corroborate our hypotheses that a misalignment of the L5 cranial adjacent vertebra after TDR leads to a reduced RoM and to high forces in the facet joints or facet capsules. Persistent high facet joint forces or facet capsule forces might induce the progression of FJD. Thus, the numerical results are able to explain the clinical results described by Siepe et al. [7].

The center of rotation of a segment after total disc replacement is defined by the fixed center of rotation of the implant which is located in the caudal vertebral body (Fig. 1). During flexion the cranial vertebra rotates around this center and thus the facet joint gap increases.

The sensitivity study showed that the misalignment of the cranial vertebra adjacent to a TDR is the main reason for high facet joint and high facet capsule forces. For the tensile forces in the facet capsule, the spinal shape, the resection of the posterior annulus, and the posterior longitudinal ligament may explain only up to 18 % of the variance (Table 2).

This study has some limitations. The results for a TDR are only presented at level L5/S1; however, we found very similar results for a TDR at level L4/L5. More than 60 % of TDRs are inserted at level L5/S1 [7]. Furthermore, only single-level TDR is investigated in this study. In addition to the misalignment, only three additional parameters were varied in this study, although there are additional

characteristics, which differ among patients. In particular, segmental distraction during insertion of the implant, the material properties of the various tissues, and the various morphologies of the facet joints were not varied in this study. The employed model was validated for the used set of material properties and achieved good agreement with experimental data [8–10]. The facet joint forces in the employed basic model were validated with measurements performed by Wilson et al. [25]. This group measured facet joint forces for lumbar specimens loaded with 7.5 Nm in extension and axial rotation in the ranges of 9–48 N and 53–109 N, respectively, and the predicted model forces agree well with these measurements and lie in the range of 15–44 N and 50–83 N for the respective loads. To account for patient individuality, five different spinal shapes were included in this study. TDR with only a fixed center of rotation was investigated here.

Pure moments and no axial compression force were applied in this study. Generally, an axial compression force on the lumbar spine causes a bending moment depending on the lever arm between the force and the center of rotation. In contrast, an optimized follower load path passes through the centers of rotation and thus causes no bending and intervertebral rotation [26]. However, when the center of rotation is varied due to a misalignment of the vertebrae, the follower load already creates a bending of the spine without any applied moment. An ideal ball-and-socket joint cannot transfer any bending moments. Thus, a follower load would lead to an additional intersegmental rotation at the index level, depending on the magnitude of the misalignment, which may lead to a misinterpretation of results due to a superimposed rotation.

In conclusion, in a probabilistic finite element study, it could be shown that an anterior displacement of the vertebra cranial to a TDR with a ball-and-socket joint leads to high facet joint forces and a posterior displacement to high facet capsule forces at the index level. A misalignment also reduced the RoM at that level. These results may explain the progression of FJD often found after TDR. In an associated clinical study [30], these findings are validated.

Acknowledgments Finite element analyses were performed at the Norddeutscher Verbund für Hoch- und Höchstleistungsrechnen (HLRN).

Conflict of interest The authors have no conflicts of interest.

References

1. Delamarter RB, Fribourg DM, Kanim LE, Bae H (2003) ProDisc artificial total lumbar disc replacement: introduction and early results from the United States clinical trial. *Spine* 28:S167–S175
2. Guyer RD, McAfee PC, Banco RJ, Bitan FD, Cappuccino A, Geisler FH, Hochschuler SH, Holt RT, Jenis LG, Majd ME, Regan JJ, Tromanhauser SG, Wong DC, Blumenthal SL (2009) Prospective, randomized, multicenter Food and Drug Administration investigational device exemption study of lumbar total disc replacement with the CHARITE artificial disc versus lumbar fusion: five-year follow-up. *Spine J* 9:374–386
3. Hochschuler SH, Ohnmeiss DD, Guyer RD, Blumenthal SL (2002) Artificial disc: preliminary results of a prospective study in the United States. *Eur Spine J* 11(Suppl 2):S106–S110
4. Sasso RC, Foulk DM, Hahn M (2008) Prospective, randomized trial of metal-on-metal artificial lumbar disc replacement: initial results for treatment of discogenic pain. *Spine* 33:123–131
5. Park CK, Ryu KS, Jee WH (2008) Degenerative changes of discs and facet joints in lumbar total disc replacement using ProDisc II: minimum two-year follow-up. *Spine* 33:1755–1761
6. Shim CS, Lee SH, Shin HD, Kang HS, Choi WC, Jung B, Choi G, Ahn Y, Lee S, Lee HY (2007) CHARITE versus ProDisc: a comparative study of a minimum 3-year follow-up. *Spine* 32:1012–1018
7. Siepe CJ, Zelenkov P, Sauri-Barraza JC, Szeimies U, Grubinger T, Tepass A, Stabler A, Mayer MH (2010) The fate of facet joint and adjacent level disc degeneration following total lumbar disc replacement: a prospective clinical, X-ray, and magnetic resonance imaging investigation. *Spine* 35:1991–2003
8. Rohlmann A, Burra NK, Zander T, Bergmann G (2007) Comparison of the effects of bilateral posterior dynamic and rigid fixation devices on the loads in the lumbar spine: a finite element analysis. *Eur Spine J* 16:1223–1231
9. Zander T, Rohlmann A, Bergmann G (2009) Influence of different artificial disc kinematics on spine biomechanics. *Clin Biomech* 24:135–142
10. Zander T, Rohlmann A, Calisse J, Bergmann G (2001) Estimation of muscle forces in the lumbar spine during upper-body inclination. *Clin Biomech* 16:S73–S80
11. Panjabi MM, Oxland T, Takata K, Goel V, Duranceau J, Krag M (1993) Articular facets of the human spine quantitative three-dimensional anatomy. *Spine* 18:1298–1310
12. Sharma M, Langrana NA, Rodriguez J (1995) Role of ligaments and facets in lumbar spinal stability. *Spine* 20:887–900
13. Eberlein R, Holzapfel GA, Schulze-Bauer CAJ (2000) An anisotropic model for annulus tissue and enhanced finite element analysis of intact lumbar disc bodies. *Comp Meth Biomech Biomed Eng* 4:209–229
14. Nolte LP, Panjabi MM, Oxland TR (1990) Biomechanical properties of lumbar spinal ligaments. In: Heimke G, Soltesz U, Lee AJC (eds) *Clinical Implant Materials. Advances in Biomaterials*, Elsevier, pp 663–668
15. Rohlmann A, Zander T, Schmidt H, Wilke H-J, Bergmann G (2006) Analysis of the influence of disc degeneration on the mechanical behaviour of a lumbar motion segment using the finite element method. *J Biomech* 39:2484–2490
16. Shirazi-Adl A, Ahmed AM, Shrivastava SC (1986) Mechanical response of a lumbar motion segment in axial torque alone and combined with compression. *Spine* 11:914–927
17. Roussouly P, Gollogly S, Berthonnaud E, Dimnet J (2005) Classification of the normal variation in the sagittal alignment of the human lumbar spine and pelvis in the standing position. *Spine* 30:346–353
18. Rohlmann A, Mann A, Zander T, Bergmann G (2009) Effect of an artificial disc on lumbar spine biomechanics: a probabilistic finite element study. *Eur Spine J* 18:89–97
19. Rohlmann A, Zander T, Bock B, Bergmann G (2008) Effect of position and height of a mobile core type artificial disc on the biomechanical behaviour of the lumbar spine. *Proc Inst Mech Eng [H]* 222:229–239

20. Zander T, Rohlmann A, Bergmann G (2006) Comparison of conventional and kinematic modeling of an artificial disc. In: 7th international symposium on computer methods in biomechanics and biomedical engineering. Antibes Juan Les Pins, France
21. Gurdak JJ, McCray JE, Thyne G, Qi SL (2007) Latin hypercube approach to estimate uncertainty in ground water vulnerability. *Ground Water* 45:348–361
22. Rohlmann A, Zander T, Rao M, Bergmann G (2009) Realistic loading conditions for upper body bending. *J Biomech* 42: 884–890
23. Dreischarf M, Rohlmann A, Bergmann G, Zander T (2011) Optimised loads for the simulation of axial rotation in the lumbar spine. *J Biomech* 44:2323–2327
24. Dreischarf M, Rohlmann A, Bergmann G, Zander T (2012) Recommended loads for the simulation of lateral bending in the lumbar spine: an optimisation finite element study. *Med Eng Phys* 34:777–780
25. Wilson DC, Niosi CA, Zhu QA, Oxland TR, Wilson DR (2006) Accuracy and repeatability of a new method for measuring facet loads in the lumbar spine. *J Biomech* 39:348–353
26. Dreischarf M, Zander T, Bergmann G, Rohlmann A (2010) A non-optimized follower load path may cause considerable inter-vertebral rotations. *J Biomech* 43:2625–2628
27. Rohlmann A, Zander T, Bergmann G (2006) Spinal loads after osteoporotic vertebral fractures treated by vertebroplasty or kyphoplasty. *Eur Spine J* 15:1255–1264
28. Ueno K, Liu YK (1987) A three-dimensional nonlinear finite element model of lumbar intervertebral joint in torsion. *J Biomech Eng* 109:200–209
29. Dooris AP, Goel VK, Grosland NM, Gilbertson LG, Wilder DG (2001) Load-sharing between anterior and posterior elements in a lumbar motion segment implanted with an artificial disc. *Spine* 26:E122–E129
30. Strube P, Hoff E, Schmidt H, Dreischarf M, Rohlmann A, Putzier M (submitted) Parameters influencing the outcome after total disc replacement at the lumbosacral junction. Part 2: distraction and retrolisthesis lead to clinical failure after a mean follow-up of 5 years. *Eur Spine J* (under review)